© 2019. Published by The Company of Biologists Ltd | Journal of Cell Science (2019) 132, jcs228478. doi:10.1242/jcs.228478

RESEARCH ARTICLE

Dkk1 exacerbates doxorubicin-induced cardiotoxicity by inhibiting the Wnt/β-catenin signaling pathway

Liying Liang[1,2], Yalin Tu[1], Jing Lu[1,2,*], Panxia Wang[1,2], Zhen Guo[1,2], Qianqian Wang[1,2], Kaiteng Guo[1,2], Rui Lan[1,2], Hong Li[3] and Peiqing Liu[1,2,*]

ABSTRACT

The cancer clinical therapy of doxorubicin (Dox) treatment is limited by its life-threatening cardiotoxic effects. Dickkopf-1 (Dkk1), the founding and best-studied member of the Dkk family, functions as an antagonist of canonical Wnt/β-catenin. Dkk1 is considered to play a broad role in a variety of biological processes, but its effects on Dox-induced cardiomyopathy are poorly understood. Here, we found that the level of Dkk1 was significantly increased in Dox-treated groups, and this increase exacerbated Dox-induced cardiomyocyte apoptosis and mitochondrial dysfunction. Overexpressing Dkk1 aggravated Dox-induced cardiotoxicity in H_9C_2 cells. Similar results were detected when adding active Dkk1 protein extracellularly. Conversely, adding specific antibody blocking extracellular Dkk1 attenuated the cardiotoxic response to Dox. Adenovirus encoding Dkk1 was transduced through intramyocardial injection and exacerbated Dox-induced cardiomyocyte apoptosis, mitochondrial damage and heart injury *in vivo*. Furthermore, Wnt/β-catenin signaling was inhibited during Dox-induced cardiotoxicity, and the re-activation of β-catenin prevented the effect of overexpressed Dkk1 and Dox-induced cardiotoxicity. In conclusion, these results reveal the crucial role of the Dkk1–Wnt/β-catenin signaling axis in the process of Dox-induced cardiotoxicity and provide novel insights into the potential mechanism of cardiomyopathy caused by clinical application of Dox.

KEY WORDS: Dkk1, Doxorubicin, Cardiomyopathy, Apoptosis, Mitochondria, Wnt/β-catenin

INTRODUCTION

Doxorubicin (Dox) is one of the most highly effective anti-cancer agents available for a wide range of malignancies, including breast cancer, osteosarcoma and Hodgkin's lymphomas. However, the major adverse effect of Dox is cardiotoxicity, which restricts its clinical application (Chatterjee et al., 2010). Many factors are involved in the pathogenesis of Dox-induced cardiotoxicity, including apoptosis, mitochondrial dysfunction and the accumulation of reactive oxygen species (ROS) (Octavia et al., 2012; Takemura and Fujiwara, 2007; Zhou et al., 2001). At present, the ameliorative effects of prevailing drugs used to treat Dox cardiomyopathy are unsatisfactory (Gianni et al., 2008; Takemura and Fujiwara, 2007), and the exact mechanism through which Dox acts needs to be further investigated.

[1]Laboratory of Pharmacology and Toxicology, School of Pharmaceutical Sciences, Sun Yat-sen University, Guangzhou 510006, P. R. China. [2]Guangdong Provincial Key Laboratory of New Drug Design and Evaluation, Sun Yat-sen University, Guangzhou 510006, P. R. China. [3]Department of Biochemistry and Molecular Biology, Guangzhou University of Chinese Medicine, Guangzhou, Guangdong, 510006, P. R. China.

*Authors for correspondence (liupq@mail.sysu.edu.cn; lujing0504@126.com)

P.L., 0000-0003-4388-2173

Received 2 December 2018; Accepted 9 April 2019

The Dickkopf (Dkk) family of secretory glycoproteins, comprises four main members (Dkk1, Dkk2, Dkk3 and Dkk4) (Niehrs, 2006). Dkk1, the founding member of Dkk family, is best studied and functions as an antagonist of canonical Wnt/β-catenin signaling pathway. Dkk1 is involved in many physiological and pathological processes, and exerts an important role in the development of many diseases (Huang et al., 2018). It has been reported that Dkk1 promoted ischemia-induced DNA damage by downregulating basal LRP5 and LRP6 (LRP5/6) levels and then altering G-protein-coupled receptor (GPCR) signals (Wo et al., 2016). Overexpression of Dkk1 led to a lack of heart looping and blood regurgitation, and a block in endocardial cushion formation because endogenous Wnt/β-catenin signaling is inhibited (Hurlstone et al., 2003). Dkk1 also served as an atherogenic factor and enhanced the endothelial–mesenchymal transition in primary aortic endothelial cells (Cheng et al., 2013; Kim et al., 2011; Ueland et al., 2009). However, the function of Dkk1 in Dox-induced cardiomyopathy remains largely unexplored.

The canonical Wnt/β-catenin signaling pathway is essential in a multitude of developmental processes and for the maintenance of homeostasis via cell proliferation and migration, apoptosis, and genetic stability and instability (Kahn, 2014; Nusse and Clevers, 2017). β-catenin is the main factor modulating in this pathway, and its stabilization leads to activation of canonical Wnt cascade. The abnormal regulation of Wnt/β-catenin pathway is associated with a variety of cardiovascular diseases. The canonical Wnt/β-catenin signaling pathway is indispensable for heart development (Andersen et al., 2018; Foulquier et al., 2018; Merks et al., 2018; Sadahiro et al., 2018). Deficiency of β-catenin leads to a failure in the differentiation of cardiac components and heart regeneration (Ozhan and Weidinger, 2015; Ruiz-Villalba et al., 2016). Wnt/β-catenin signaling is also important to prevent cardiac senescence caused by Dox cardiotoxicity (Xie et al., 2018).

This present study sought to investigate whether the Dkk1–Wnt/β-catenin signaling axis plays a role in the process of Dox-induced cardiomyopathy. We found that both overexpressing Dkk1, via infection with adenovirus (Ad-Dkk1), and adding of active Dkk1 protein aggravated Dox-induced apoptosis, mitochondrial injury and cardiac dysfunction by inhibiting the canonical Wnt/β-catenin signaling pathway. Conversely, extracellular addition of specific anti-Dkk1 antibody attenuated Dox-induced cardiotoxicity. This might be helpful to better understand the mechanism of Dox-induced cardiomyopathy and provide a potential therapy for the detrimental effects of Dox treatment.

RESULTS

Dkk1 is upregulated during Dox-induced cardiotoxicity in H_9C_2 cells

To detect the changes in Dkk1 during Dox-induced cardiotoxicity, rat embryonic ventricular myoblastic H_9C_2 cells were treated with

Journal of Cell Science (2019) 132, jcs228478. doi:10.1242/jcs.228478

Dox (1 μmol/l) for the times indicated. As shown in Fig. 1A–C, Dox treatment significantly reduced the cell viability and increased the proportion of cells undergoing apoptosis at 12 h, as implied by morphological changes, and MTS assay and flow cytometry analysis. Western blotting results showed that Dox caused an increase in apoptosis biomarkers (Bax relative to Bcl2, cleaved caspase 3 relative to total caspase 3, and cleaved PARP1 relative to total PARP1) (Fig. 1D,E). In addition, Dox induced the decline of mitochondrial membrane potential (by Rh123 and TMRE staining), as well as nuclear condensation (as determined by Hoechst 33342

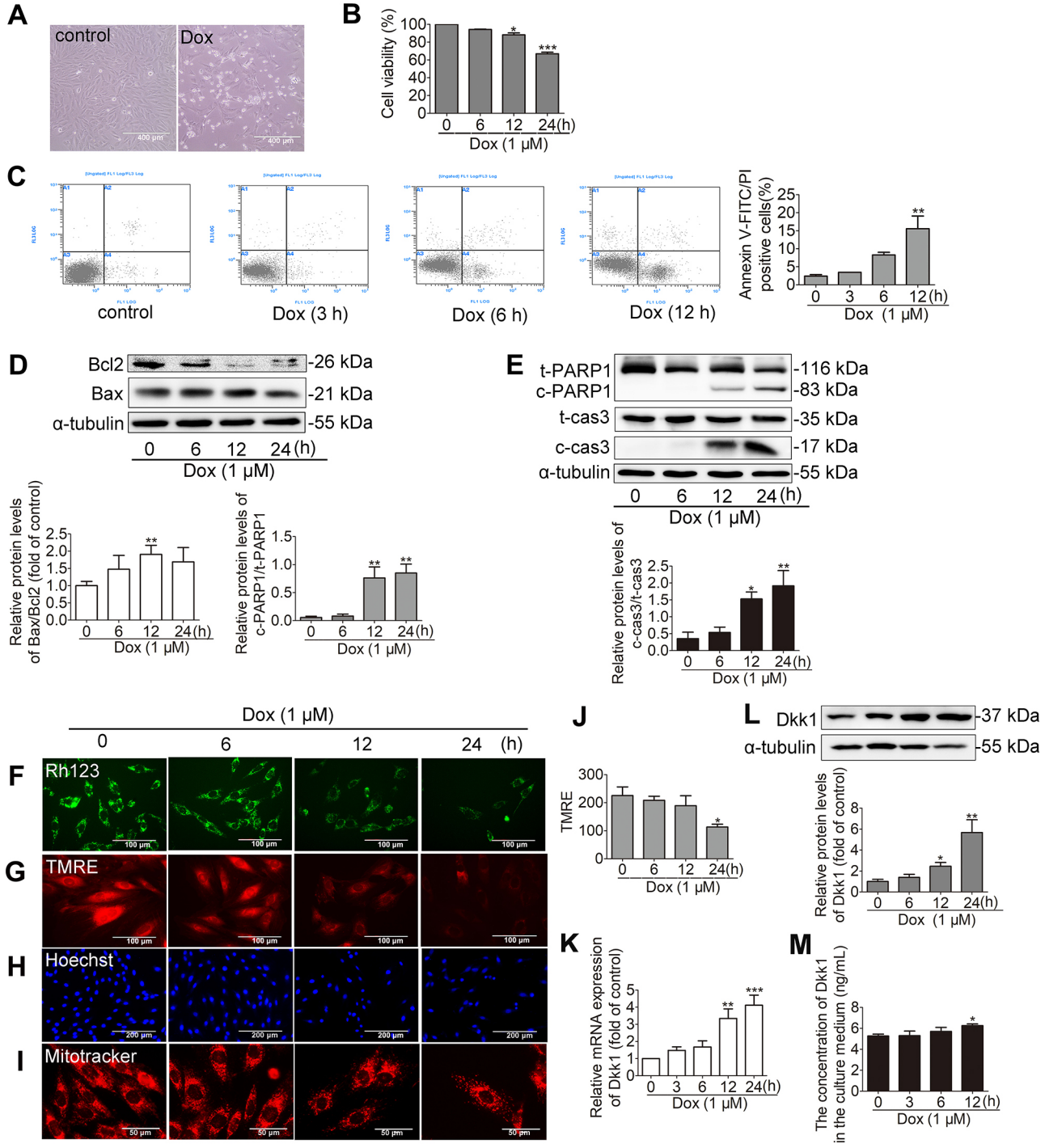

Fig. 1. Dkk1 expression is upregulated by Dox treatment *in vitro*. H_9C_2 cells were incubated with 1 μmol/l Dox for the indicated time. (A) The morphology of cells was shown after 12 h incubation of Dox. (B,C) The cell viability (B) and proportion of apoptotic cells (C) were measured by MTS assay and flow cytometric analysis. (D,E) The relative protein levels of Bax to Bcl2 (D), and cleaved caspase 3 (c-cas3) to total caspase 3 (t-cas3), and cleaved (c)-PARP1 to total (t)-PARP1 (E) were determined by western blot analysis. (F–J) Rh123 and TMRE, Hoechst 33342 and Mitotracker staining were conducted to determine $\Delta\psi_m$, nuclear condensation and mitochondrial morphology, respectively. (K–M) The mRNA (K), protein levels (L) and extracellular concentration (M) of Dkk1 were measured by qRT-PCR, western blotting and ELISA assays, respectively. In L, the lane order in the western blot matches that shown in the graph underneath. The results were normalized to levels of β-actin (mRNA) and α-tubulin (protein) and are presented as means±s.e.m., n=5. *P<0.05, **P<0.01, ***P<0.001 versus control group.

Journal of Cell Science

Journal of Cell Science (2019) 132, jcs228478. doi:10.1242/jcs.228478

staining) and mitochondrial matrix swelling/disorganization (by Mitotracker staining) (Fig. 1F–J). The results from quantitative real-time RT-PCR (qRT-PCR) and western blot analysis suggested that the mRNA and protein expression of Dkk1 was remarkably increased after exposure to Dox for 12 h (Fig. 1K,L). Compared with the control group, an increase in the Dkk1 protein concentration was discovered in the culture medium after 12 h Dox treatment through an ELISA assay (Fig. 1M), suggesting that Dox promoted the Dkk1 secretion process.

The changes in Dkk1 during Dox-induced cardiotoxicity in the hearts of SD rats

To further assess the changes in Dkk1 during Dox-induced cardiomyopathy *in vivo*, SD rats were intraperitoneally injected with three equal doses (each containing 5 mg/kg body weight) every 4 days with a total cumulative dose of 15 mg/kg body weight Dox, and the control group received the same volume of normal saline in parallel. The hearts of Dox-treated rats were obviously smaller than those of control group (Fig. 2A). Hematoxylin and eosin (HE), Masson and Picro Sirius Red (PSR) staining revealed that Dox treatment also increased the disorganization of myoctyes and cardiac fibrosis (Fig. 2B–D; Fig. S1A). The heart weight to the tibia length ratio (HW:TL) was obviously decreased in the Dox group (Fig. 2F). Echocardiography illustrated a tendency of decrease in ejection fraction (EF %), fractional shortening (FS %), stroke volume (SV), cardiac output (CO), interventricular septum (IVS), left ventricular posterior wall thickness (LVPW), left ventricular diameter (LVID) and left ventricular volume (LVV) for Dox-treated rats (Fig. 2E,G–O). Western blot analysis and Tunel staining showed that the proportion of apoptotic cardiomyocytes was significantly increased in the Dox group (Fig. 2P,Q). Moreover, we detected that these were abnormal structural changes in the nucleus (such as condensation and paramorphia) and mitochondria (including irregular arrangement, swelling, vacuolation and disrupted cristae) in Dox-treated rat hearts by using transmission electron microscopy (TEM) (Fig. 2S). All of these results show the model of Dox-induced cardiomyopathy had been successfully established *in vivo*. In accordance with results from H_9C_2 cells, Dox injection remarkably increased the mRNA and protein levels of Dkk1 (Fig. 2R,T,U). We also determined that Dox induced the secretion of Dkk1 into the serum (Fig. 2V).

Involvement of Dkk1 in Dox-induced cardiotoxicity in H_9C_2 cells

To investigate whether Dkk1 plays a role in Dox-induced cardiotoxicity, recombinant adenovirus was used to overexpress Dkk1 (Ad-Dkk1) in H_9C_2 cells. As shown in Fig. 3A–G, overexpressing Dkk1 exacerbated Dox-induced cardiomyocyte apoptosis, mitochondrial membrane depolarization, nuclear condensation and mitochondria swelling. Given that Dox treatment promoted Dkk1 protein secretion extracellulary (Fig. 2V), we added active Dkk1 protein or anti-Dkk1 antibody (hereafter anti-Dkk1) to culture medium to explore the role of extracellular Dkk1 in Dox-induced cardiotoxicity. The active Dkk1 protein aggravated Dox-induced cardiomyocyte apoptosis and mitochondrial disorder (Fig. 3H–L). Conversely, extracellular addition of anti-Dkk1 attenuated Dox-induced apoptosis and mitochondrial dysfunction (Fig. 3M–Q). In addition, treatment with the Dkk1 inhibitor [WAY-262611 (WAY) at 1.25 µmol/l for 48 h] reversed the effects of Ad-Dkk1 in Dox treatment (Fig. 3R). These results suggested that extracellular Dkk1 aggravated Dox-induced cardiotoxicity.

Overexpression of Dkk1 exacerbates Dox-induced cardiomyocyte apoptosis, mitochondrial injury and heart injury *in vivo*

Adenovirus encoding Dkk1 was transduced into the rat left ventricle through intramyocardial injection. After 14 days, we performed another 2-week Dox treatment; this gives a total *in vivo* overexpression duration of 28 days. Compared with the Ad-GFP group, the mRNA expression, the intracellular and serum protein levels of Dkk1 were obviously increased in the Ad-Dkk1 overexpression rats (Fig. 4A–C), suggesting that Dkk1 protein was successfully overexpressed in the Ad-Dkk1 group. The heart size of rats with Dox treatment was much smaller than in those overexpressing Dkk1 (Fig. 4D). The myocyte disorganization and fibrosis induced by Dox was worse in the hearts of Ad-Dkk1-treated rats, as shown by HE, Masson and PSR staining (Fig. 4E–G). There was no significant difference in heart weight (HW), body weight (BW) and tibia length (TL) between Ad-Dkk1 overexpression plus Dox treatment and Dox-treated rats (Fig. 4H–J). However, the HW:TL ratio was distinctly reduced after Ad-Dkk1 overexpression in the Dox-treated group (Fig. 4K). The echocardiography data revealed that both Ad-Dkk1 and Dox treatment caused cardiac dysfunction, and overexpression of Dkk1 exacerbated Dox-induced heart injury (Fig. 5A–I; Fig. S2). In addition, the level of apoptosis was exacerbated when rats were infected with Dkk1, as revealed through a Tunel assay and western blot analysis (Fig. 5J,K). As shown in TEM images, the delivery of Ad-Dkk1 exacerbated Dox-induced damage of nuclei and mitochondria (Fig. 5L).

Dkk1 aggravated Dox-induced cardiotoxicity via inhibiting canonical Wnt/β-catenin signaling pathway

As it has been reported that Dkk1 is an inhibitor of the canonical Wnt/β-catenin signaling pathway (Huang et al., 2018), we determined the β-catenin level after Dox treatment and found that the protein expression of β-catenin was downregulated in Dox-treated H_9C_2 cells and heart tissues (Fig. 6A,B). To determine the role of the canonical Wnt/β-catenin signaling pathway in Dox-induced cardiomyopathy, cells were pre-treated with a specific activator of β-catenin (LiCl) or its inhibitor [KYA1797K (KYA)] followed by Dox for 12 h. As shown in Fig. 6C–F, LiCl suppressed the protein expression of apoptosis biomarkers, and reduced the level of Dox-induced apoptosis in cardiomyocytes. By contrast, KYA exacerbated the Dox-triggered cardiotoxicity response (Fig. 6G–J). Furthermore, active Dkk1 protein reduced the protein expression of β-catenin, while anti-Dkk1 alleviated the downregulation of β-catenin caused by Dox (Fig. 7A,B). Dkk1 overexpression aggravated the Dox-induced reduction in β-catenin protein levels, and the Dox-induced increase in apoptosis and mitochondrial damage, which was reversed by treatment with the β-catenin activator LiCl (Fig. 7C–I). These results suggested that Dkk1 aggravates Dox-induced cardiotoxicity via inhibiting canonical Wnt/β-catenin signaling pathway.

DISCUSSION

Dox is an effective chemotherapy drug for many tumors, but its clinical application is limited by its serious cardiotoxicity (Chatterjee et al., 2010). The pathological characteristics of Dox-induced cardiotoxicity are similar to those of dilated cardiomyopathy, including cardiomyocyte apoptosis, mitochondrial swelling, energy metabolism abnormality and excessive accumulation of ROS (Green and Leeuwenburgh, 2002; Santulli et al., 2015; Štěrba et al., 2013; Umanskaya et al., 2014; Zhou et al., 2001). Existing drugs focusing on reduction of ROS accumulation fail to reverse this side effect

Journal of Cell Science (2019) 132, jcs228478. doi:10.1242/jcs.228478

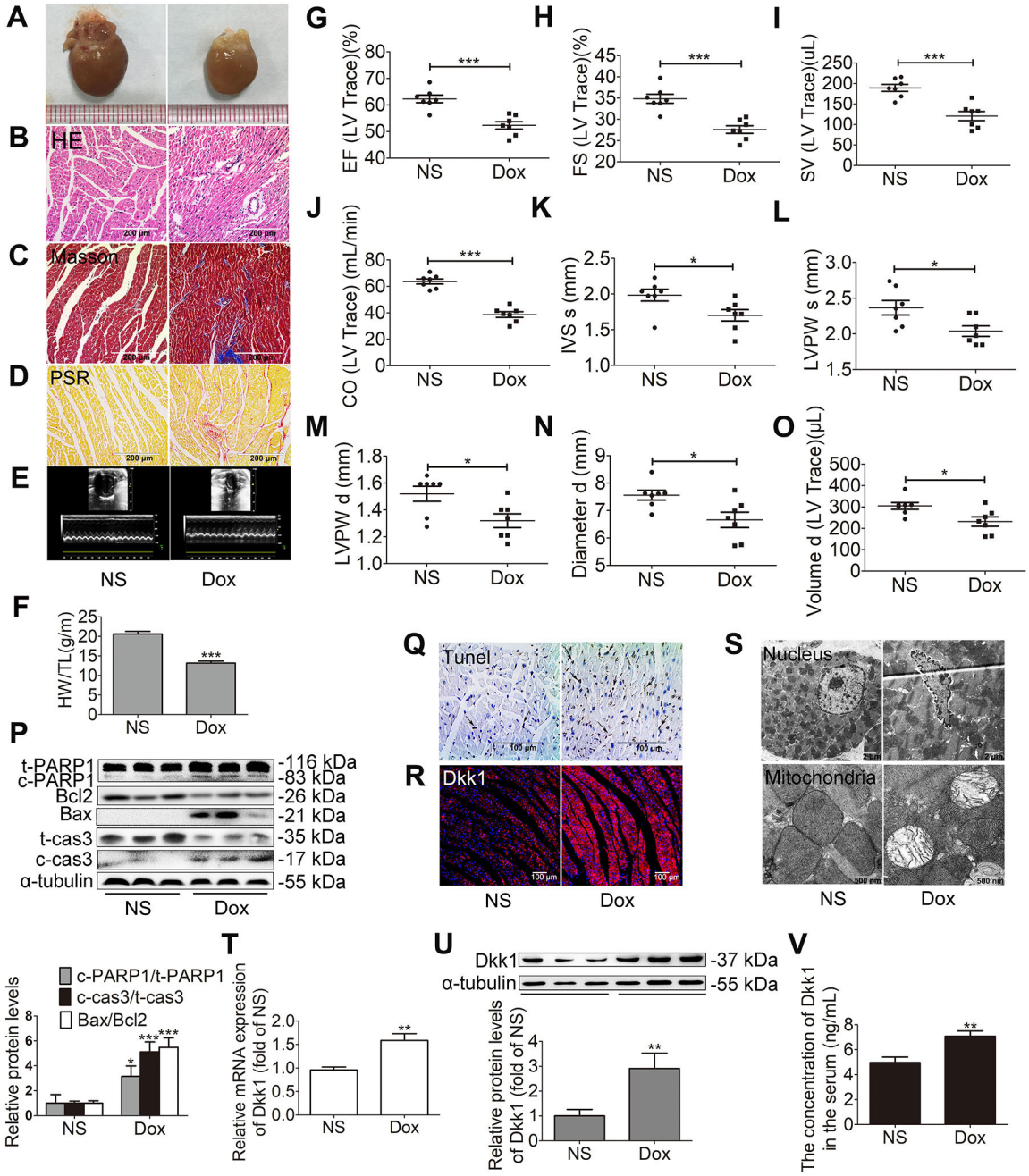

Fig. 2. Changes of Dkk1 in Dox-induced cardiotoxicity *in vivo*. Sprague-Dawley (SD) rats were given intraperitoneal injections with a total cumulative dose of 15 mg/kg body weight Dox or an equal volume of normal saline (NS), n=6. (A) The gross hearts of two groups are shown. Scale ruler has 1 mm intervals. (B–D) HE (B), Masson (C) and Picro Sirius Red (PSR) staining (D) are presented, showing pathological changes in heart tissues. Scale bars: 200 μm. (E,G–O) Representative echocardiographic graphs (E) and functional parameters [ejection fraction (EF %), fractional shortening (FS %), stroke volume (SV), cardiac output (CO), interventricular septum (IVS), left ventricular posterior wall thickness (LVPW), left ventricular diameter (LVID) and left ventricular volume (LVV)] were determined (G–O). (F) The heart mass to the tibia length ratio (HW/TL) between two groups. (P) The levels of the apoptosis biomarkers [relative protein levels of Bax to Bcl2, cleaved caspase 3 (c-cas3) to total caspase 3 (t-cas3) and cleaved (c)-PARP1 to total (t)-PARP1] were analyzed by western blotting. (Q,R) Tunel staining (Q) and immunofluorescence (R) were used to detect DNA fragmentation of apoptotic cells and the level of Dkk1, respectively. Scale bars: 100 μm. (S) Structural changes in the nucleus and mitochondria were assessed through TEM imaging. Scale bars: 2 μm (nucleus), 500 nm (mitochondria). (T–V) The mRNA (T), protein levels (U) and circulating concentration of Dkk1 (V) were determined by qRT-PCR, western blotting and ELISA assay, respectively. In U, the left three lanes in the western blot are for the NS group and the right are for the Dox group. The data represents means±s.e.m. *P<0.05, **P<0.01, ***P<0.001 versus the NS group.

(Gianni et al., 2008; Takemura and Fujiwara, 2007), suggesting that the mechanism of Dox-induced cardiomyopathy is very complicated, with contributions from multiple factors and pathways, and deserves further study (Hulmi et al., 2018; Li et al., 2018; Yarana et al., 2018). In this study, we found that both overexpressing Dkk1, through infection of Ad-Dkk1, and the addition of active Dkk1 protein aggravated Dox-induced apoptosis, mitochondrial injury and cardiac dysfunction. Conversely, extracellular addition of specific anti-Dkk1 antibody attenuated Dox-induced apoptosis and mitochondrial damage. Knockdown of Dkk1 and treatment with the Dkk1 inhibitor WAY in H9C2 cells showed the similar effects to that of anti-Dkk1 antibody (Figs S3, S4).

Journal of Cell Science

Journal of Cell Science (2019) 132, jcs228478. doi:10.1242/jcs.228478

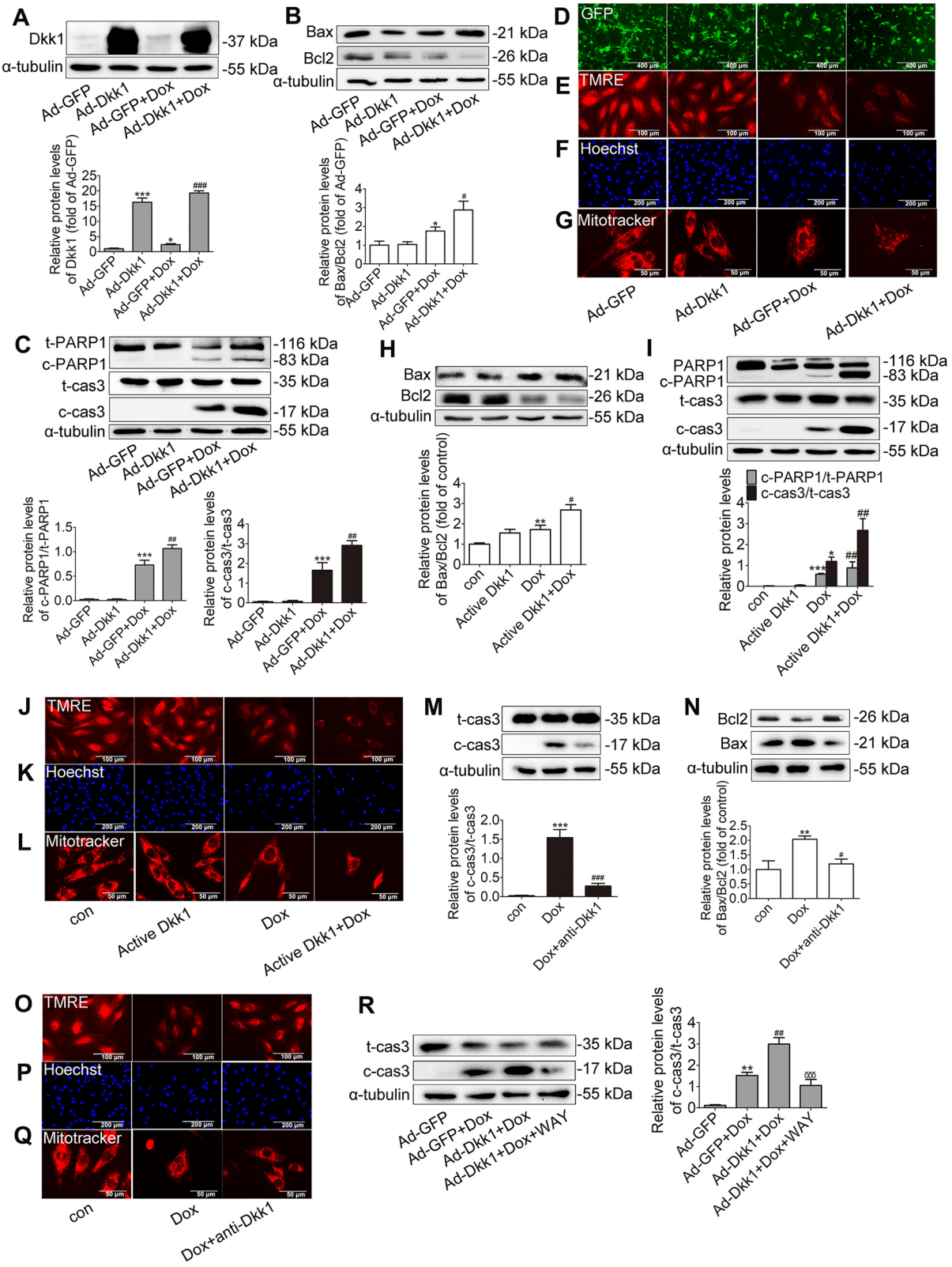

Fig. 3. See next page for legend.

Dkk1 is well known as an inhibitor of canonical Wnt/β-catenin signaling cascade, and acts by inducing endocytosis of the ternary Dkk1–LRP5/6–Kremen1 complex or by competitively binding to the Wnt co-receptor (Foulquier et al., 2018). Dkk1 destabilizes atherosclerotic lesions and promotes plaque formation and vulnerability through inhibiting Wnt signaling during atherosclerosis (Di et al., 2017). Baicalin and geniposide exerts anti-inflammation effects to prevent the development of atherosclerosis by elevating the ratio of Wnt1 to Dkk1 (Wang et al., 2016). Dkk1 induces the endocytosis and degradation of LRP5/6 to promote cardiac ischemic

Journal of Cell Science

Journal of Cell Science (2019) 132, jcs228478. doi:10.1242/jcs.228478

Fig. 3. Dkk1 is involved in Dox-induced cardiomyopathy in H_9C_2 cells. H_9C_2 cells were infected with Ad-GFP or Ad-Dkk1, and incubated with Dox for 12 h. (A) The change in Dkk1 levels was determined by western blot analysis. (B,C) The relative protein levels of Bax to Bcl2 (B), cleaved caspase 3 (c-cas3) to total caspase 3 (t-cas3) and cleaved (c)-PARP1 to total (t)-PARP1 (C) were determined by western blot analysis. (D–G) $\Delta\psi_m$, nuclear condensation and mitochondrial morphology were detected by TMRE, Hoechst 33342 and Mitotracker staining. (H–Q) Active Dkk1 protein (100 ng/ml) was added to culture medium for a 30 min pre-incubation before 12 h Dox treatment. Anti-Dkk1 antibody (diluted 1:1000) was added to culture medium during the 12 h Dox treatment when indicated. The protein levels of apoptosis biomarkers (Bax relative to Bcl2, c-cas3 relative to t-cas3 and c-PARP1 relative to t-PARP1) were determined by western blotting (H,I,M,N), and $\Delta\psi_m$, nuclear condensation and mitochondrial morphology were observed through TMRE, Hoechst 33342 and Mitotracker staining (J–L,O–Q). In H,I,M,N, the lane order in the western blots matches that shown in the graphs underneath. (R) A reduction in apoptosis markers is seen upon inclusion of WAY (1.25 µmol/l for 48 h) for the Ad-Dkk1+Dox cells, as determined by western blotting. The data represents means±s.e.m., n=5. *P<0.05, **P<0.01, ***P<0.001 versus Ad-GFP or control group; $^{\#}P$<0.05, $^{\#\#}P$<0.01, $^{\#\#\#}P$<0.001 versus Ad-GFP+Dox or Dox group; $^{\delta\delta\delta}P$<0.05 versus Ad-Dkk1+Dox group.

injury (Wo et al., 2016). It has also been found that high circulating levels of Dkk1 are related to type 2 diabetes with cardiovascular disease (Garcia-Martín et al., 2014). Here, our results show that the mRNA expression, the intracellular and serum protein levels of Dkk1 are substantially increased after exposure to Dox treatment, suggesting that Dox promotes the Dkk1 secretion process.

Canonical Wnt/β-catenin signaling is required in embryogenesis and organogenesis and for homeostasis, and participates in many disease processes, including cardiac development and cardiovascular diseases (Kahn, 2014; Nusse and Clevers, 2017). The disruption of Wnt/β-catenin signaling in epicardial cells and cardiac fibroblasts impairs cardiac function after acute ischemic cardiac injury (Duan et al., 2012). Overexpression of β-catenin decreases apoptosis and the size of myocardial infarctions (MIs), and improves ventricular function, suggesting that canonical Wnt signaling is important in MI healing (Dawson et al., 2013). The activation of Wnt signaling inhibits adipogenic transcription factors, and is beneficial to arrhythmogenic right ventricular cardiomyopathy (Dawson et al., 2013). In addition, the long intergenic noncoding RNAs (lincRNA) p21 (also known as *TRP53COR1*) exerts an anti-senescence effect on Dox-associated cardiotoxicity, while that effect is widely abolished upon silencing β-catenin (Xie et al., 2018). We found that the protein levels of β-catenin were reduced in our Dox-induced cardiotoxicity model.

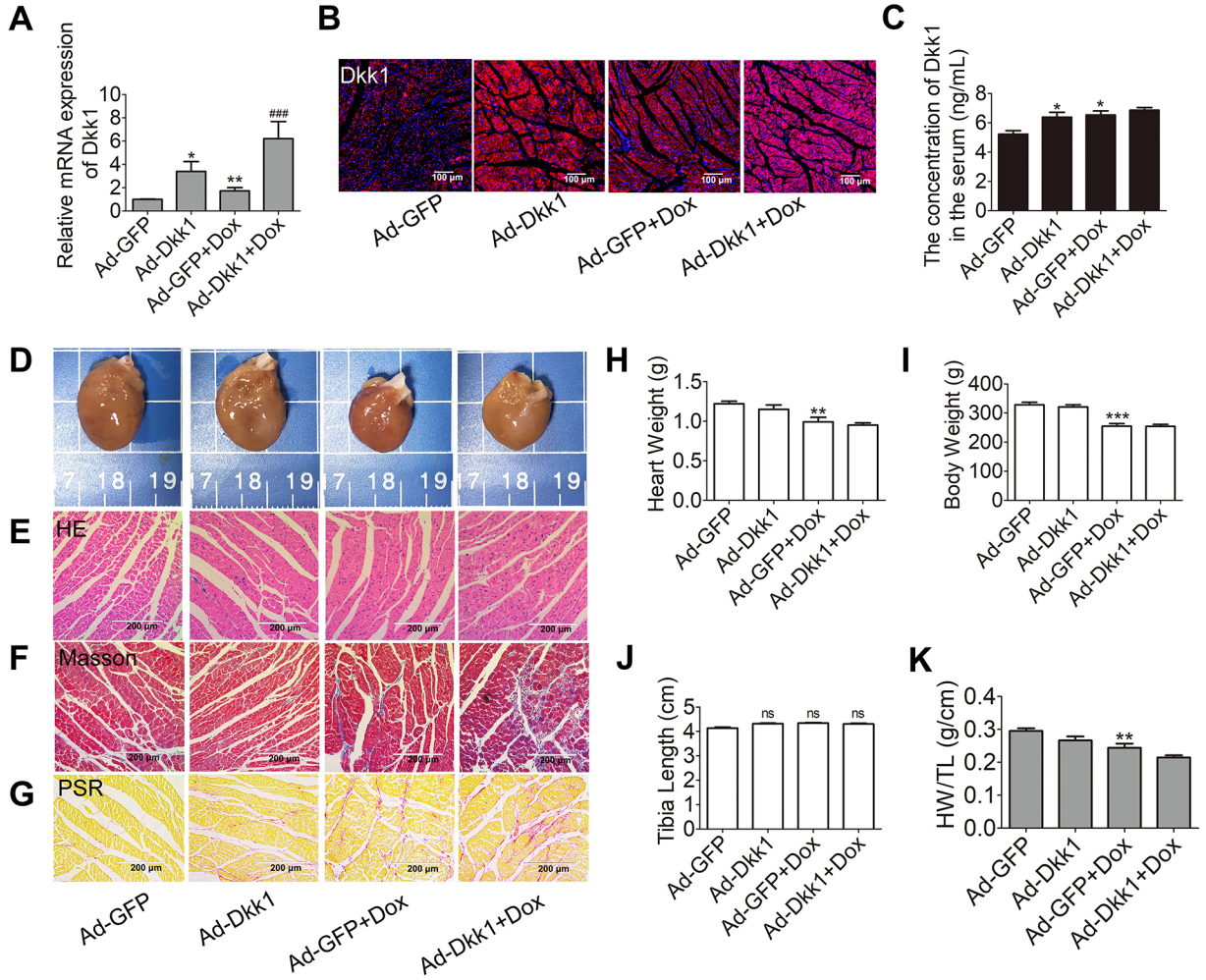

Fig. 4. Overexpression of Dkk1 promotes heart injury induced by Dox. Sprague-Dawley (SD) rats were submitted to Ad-GFP or Ad-Dkk1 intramyocardial injection and Dox intraperitoneal injection (15 mg/kg body weight), n=8–14. (A–C) The mRNA (A), protein levels (B) and circulating concentration of Dkk1 (C) were determined by qRT-PCR, immunofluorescence and ELISA assay, respectively. (D) The hearts of four groups are shown. Grid lines are at 5 mm intervals. (E–G) Pathological changes of heart tissues as observed by HE, Masson and Picro Sirius Red (PSR) staining . (H–K) Heart weight (HW), body weight (BW) and tibia length (TL), and the heart weight to the tibia length (HW/TL) ratio are shown for the indicated groups. The data represents means±s.e.m. *P<0.05, **P<0.01, ***P<0.001 versus Ad-GFP group. $^{\#\#\#}P$<0.001 versus Ad-GFP+Dox group. ns, not significant.

Journal of Cell Science (2019) 132, jcs228478. doi:10.1242/jcs.228478

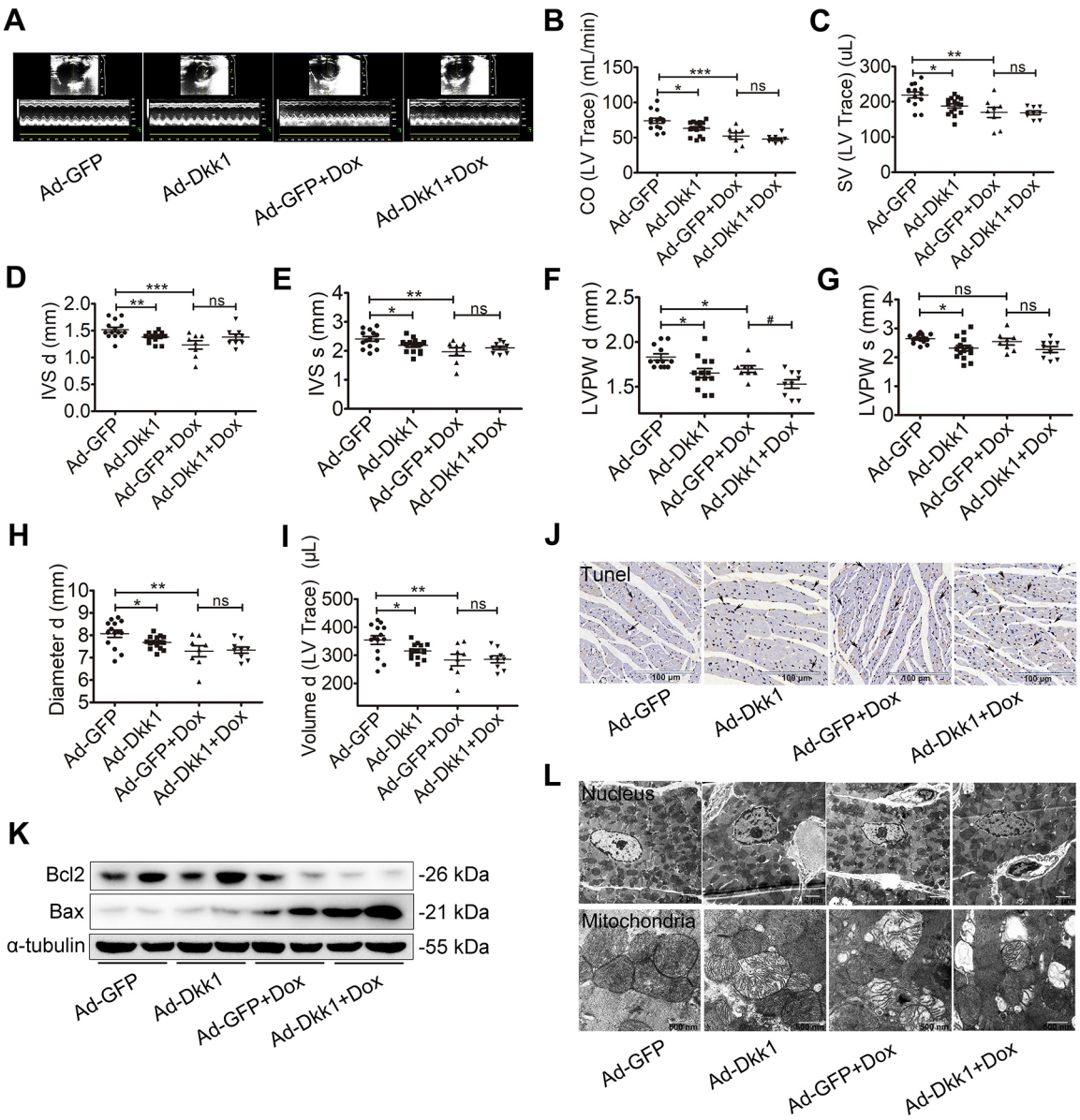

Fig. 5. Overexpression of Dkk1 exacerbates Dox-induced cardiomyocyte apoptosis and mitochondria dysfunction. (A–I) Representative echocardiographic graphs (A) and main functional parameters [cardiac output (CO), stroke volume (SV), interventricular septum (IVS), left ventricular posterior wall thickness (LVPW), left ventricular diameter (LVID) and left ventricular volume (LVV); B–I] for Sprague-Dawley (SD) rats in the four groups as in Fig. 4 are presented. (J) The level of DNA fragmentation as visualized by Tunel staining. (K,L) Western blotting and TEM were conducted to determine the protein levels of Bax and Bcl2 (K), and changes of structure in nuclear and mitochondria (L) in heart tissues. The data represents means±s.e.m., n=8–14. *P<0.05, **P<0.01, ***P<0.001 versus Ad-GFP group. $^{\#}P$<0.05 versus Ad-GFP+Dox group. ns, not significant.

Moreover, LiCl (a specific activator of β-catenin) suppressed Dox-induced cardiomyocyte apoptosis and mitochondrial injury, while KYA1797K (an inhibitor of β-catenin) exacerbated the Dox-triggered cardiotoxicity response, implying that activation of Wnt signaling has a protective effect on Dox-induced cardiomyopathy.

In view of the close relationship between Dkk1 and the canonical Wnt/β-catenin signaling pathway in cardiovascular diseases, we speculated that Wnt/β-catenin signaling was involved in the process of Dkk1 aggravated Dox-induced cardiotoxicity. Here, we found that overexpression of Dkk1 aggravated the Dox-induced reduction in β-catenin protein levels, and the Dox-induced increase in apoptosis and mitochondrial damage, which was reversed by treatment with the β-catenin activator LiCl. Dkk1 levels inversely co-related with β-catenin in cardiomyocytes, but β-catenin induction did not affect the protein expression of Dkk1 (Fig. S5).

In summary, this study uncovered that Dkk1 plays a key role in Dox-induced cardiomyopathy via inhibiting the canonical Wnt/β-catenin signaling pathway. Although there were some limitations, our study suggests that monitoring and lowering extracellular Dkk1 protein may serve as a potential therapeutic approach for cardiomyopathy caused by clinical application of Dox.

MATERIALS AND METHODS

Reagents and antibodies

Doxorubicin (Dox, purity 99.37%) was bought from TargetMol (Target Molecule Corp., USA) and was dissolved in water to 10 mmol/l and stored at −20°C. KYA1797K and WAY-262611 were obtained from MCE

Journal of Cell Science (2019) 132, jcs228478. doi:10.1242/jcs.228478

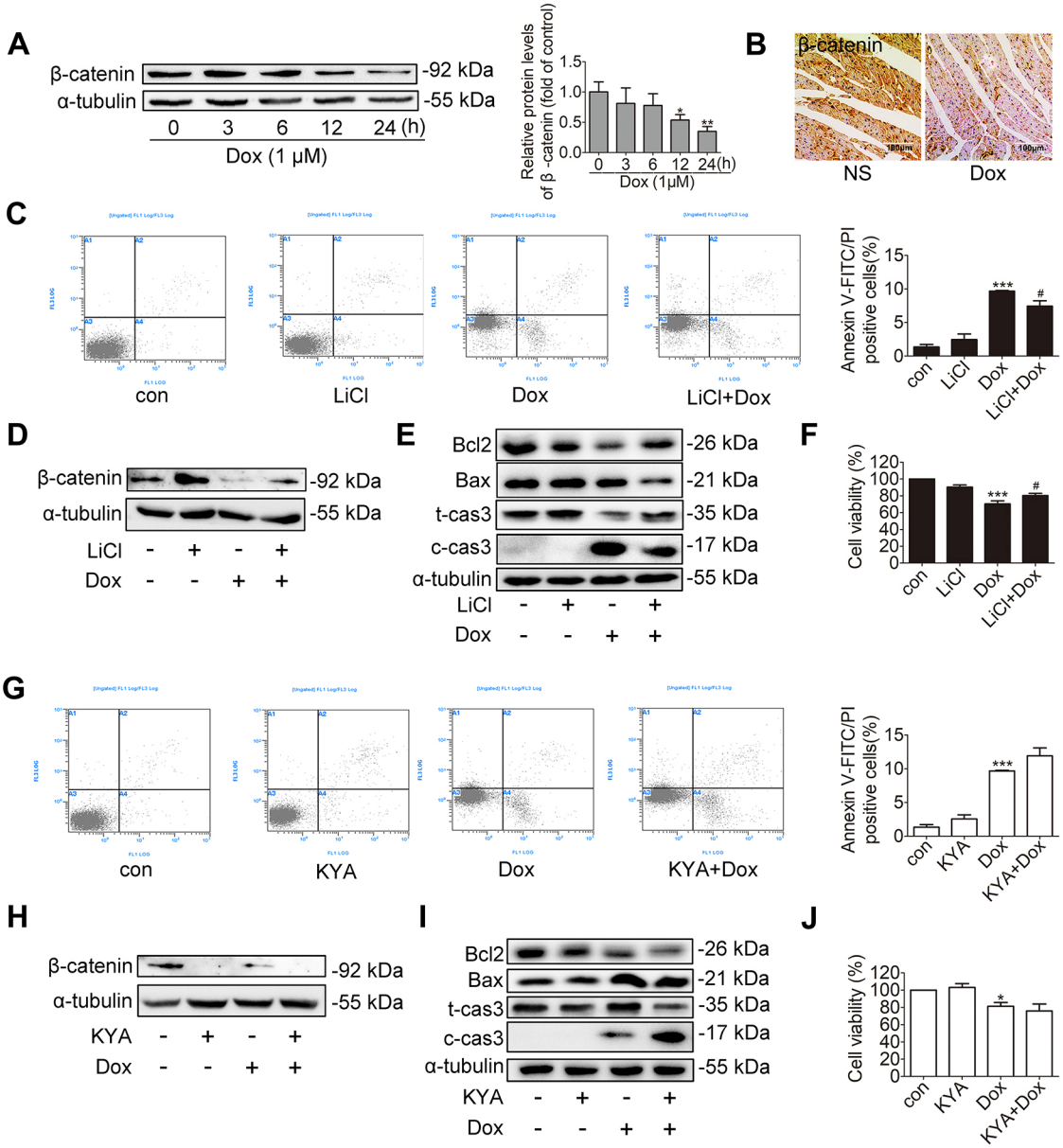

Fig. 6. The change and function of canonical Wnt/β-catenin signaling pathway during Dox-induced cardiotoxicity. (A,B) The levels of β-catenin were analyzed by western blotting for H9C2 cells, and by immunohistochemical staining for heart tissues treated as in Fig. 2. Scale bars: 100 µm. (C,G) H_9C_2 cells were pre-incubated with LiCl (20 mmol/l) or KYA1797K (5 µmol/l) before 12 h Dox treatment. Flow cytometry was used to assess the proportion of apoptotic cells for with LiCl (C) or KYA1797K (G) treatments with Dox stimulation. (D–F,H–I) The changes in the level of the apoptosis biomarkers [relative protein levels of Bax to Bcl2, cleaved caspase 3 (c-cas3) to total caspase 3 (t-cas3) and cleaved (c)-PARP1 to total (t)-PARP1] (D,E,H,I) and the cell viability (F,J) were determined by western blotting and an MTS assay. The data represents means±s.e.m., n=3. *P<0.05, **P<0.01, ***P<0.001 versus control group. $^{\#}P$<0.05 versus Dox group.

(MedChemexpress) and diluted in DMSO and stored at −80°C. The rat Dkk1 ELISA kit was from Mlbio (Shanghai, China). Primary antibodies against Dkk1 (diluted 1:3000, goat; cat. no AF4010) were purchased from R&D systems. Rabbit antibodies against caspase 3 (diluted 1:1000; cat. no 19677-1-AP) and PARP1 (diluted 1:1000; cat. no 13371-1-AP) were from Proteintech Group (Chicago, IL). Rabbit anti-cleaved caspase 3 (diluted 1:1000; cat. no 9661) and -β-catenin (diluted 1:1000; cat. no 8480) antibodies were obtained from Cell Signaling Technology. Anti-Bax (diluted 1:1000, rabbit; cat. no ab32503), Bcl2 (diluted 1:200, rabbit; cat. no BA0412) and α-tubulin (diluted 1:5000, mouse cat. no T6199) antibodies were products from Abcam and Sigma-Aldrich, respectively.

The culture of rat embryonic ventricular myoblastic H_9C_2 cells

Rat embryonic ventricular myoblastic H_9C_2 cells were received from the Cell Bank of the Chinese Academy of Sciences (CAS, Shanghai, China). The cells were maintained in Dulbecco's modified Eagle's medium (DMEM; GIBCO, Invitrogen, Carlsbad, CA) supplemented with 10% fetal bovine serum (FBS) and incubated at 37°C under 5% CO_2.

Western blot analysis

After extracting from cells or tissues, proteins were separated by SDS-PAGE and transferred onto a polyvinylidene difluoride membrane (Millipore). Afterwards, the membranes were blocked for 1 h at ∼25°C with 5% skimmed milk [dissolved in Tris-buffered saline with 0.1% Tween 20 (TBST)] and incubated with the indicated primary antibodies at 4°C overnight, followed by incubation with horseradish peroxidase-conjugated secondary antibodies for 1 h at ∼25°C. Protein bands were detected with enhanced chemiluminescent substrate, and the intensity analysis was performed by LabWorks software (Bio-Rad).

Journal of Cell Science (2019) 132, jcs228478. doi:10.1242/jcs.228478

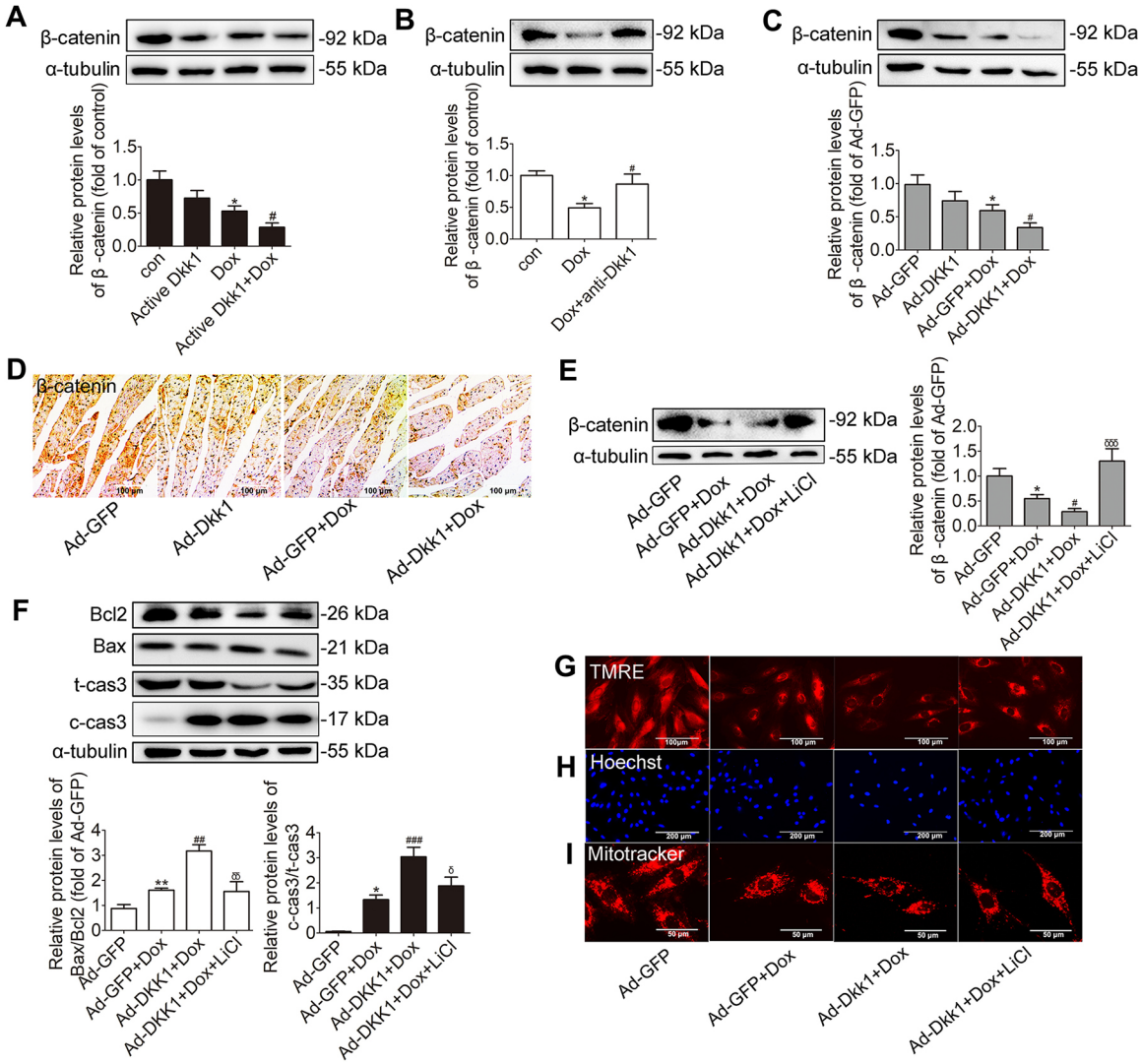

Fig. 7. Dkk1 aggravates Dox-induced cardiotoxicity by inhibiting the canonical Wnt/β-catenin signaling pathway. (A–D) Active Dkk1 protein, anti-Dkk1 antibody and Dkk1 overexpression in H9C2 cells changes the levels of β-catenin, as determined by western blotting (A–C). The expression of β-catenin in rat heart tissues was assessed by immunohistochemical staining (D). Rat hearts were treated as in Fig. 4. In A–C, the lane order in the western blots matches that shown in the graphs underneath. (E–I) Ad-Dkk1 promotes Dox-induced cardiomyocyte apoptosis and mitochondria disorganization and LiCl suppresses this change, as assessed by western blotting (E,F) and TMRE, Hoechst 33342 and Mitotracker staining (G–I) for for H9C2 cells. The data represents means±s.e.m., n=3. $^{*}P$<0.05, $^{**}P$<0.01 versus Ad-GFP or control group. $^{\#}P$<0.05, $^{\#\#}P$<0.01, $^{\#\#\#}P$<0.001 versus Ad-GFP+Dox or Dox group. $^{\delta}P$<0.05, $^{\delta\delta\delta}P$<0.001 versus Ad-Dkk1+Dox group.

qRT-PCR

RNA from H_9C_2 cells or rat cardiac tissues was isolated with Trizol reagent (Invitrogen). cDNA was then prepared with a one-step RT kit (Thermo Fisher Scientific) in 20 µl reactions. A SYBR-Green quantitative PCR kit in an iCycler iQ system (Bio-Rad) was used to detect the mRNA levels of each different gene. The amplification conditions were 15 min at 95°C, then followed by 40 cycles of 30 s at 95°C, 1 min at 55°C and 30 s at 72°C. All PCRs were performed in triplicate. Each rat-specific primer was synthesized by Sangon (Shanghai, China). β-actin was used as a housekeeping gene for normalization.

The sequences of rat-specific primers were as follows: Dkk1, 5′-CCC-TCTGACCACAGCCATTT-3′ and 5′-AGAGCCTTCTTGCCCTTTGG-3′; and β-actin, 5′-ACAACCTTCTTGCAGCTCCTC-3′ and 5′-CTGACC-CATACCCACCATCAC-3′.

Rat model, echocardiography and morphometric measurements

All animal experiments were performed according to the Guide for the Care and Use of Laboratory Animals (NIH Publication No.85-23, revised 1996) and approved by the Research Ethics Committee of Sun Yat-Sen University. Male Sprague-Dawley (SD) rats (7–8 weeks of age, weighing 180–220 g, Certification No. 44005800007189, SPF grade) were provided by the Experimental Animal Centre of Guangzhou University of Chinese Medicine. After a 3-day quarantine, 16 rats were randomized into two groups, and received Dox and normal saline (NS), respectively. Over a period of 14 days, Dox was intraperitoneally injected in three equal dosages (each containing 5 mg/kg body weight) every 4 days and the final cumulative dose was 15 mg/kg body weight. Rats in the control group received an equal volume of NS administrated in parallel.

After the 2-week treatment, two-dimensional-guided M-mode echocardiography was performed with a Technos MPX ultrasound system (ESAOTE, SpAESAOTE SpA, Italy) and the basic hemodynamic parameters were measured. Then the animals were killed and their fresh hearts were rapidly removed. For morphometric measurement, histological cross sections (5 µm thick) of the heart tissues were fixed in 4% paraformaldehyde and then treated with hematoxylin-eosin (HE), Masson and Sirus Red stain. The rest of the tissues was quickly frozen in liquid nitrogen and then stored at −80°C for further assay.

Intramyocardial delivery of recombinant Dkk1 adenovirus

SD rats were anesthetized with 7% chloral hydrate (0.35 mg/kg body weight) before endotracheal intubation. Then, left thoracotomy was

conducted to expose the heart for direct gene delivery. A total of 200 µl Ad-Dkk1 or Ad-GFP (10^9 particles) were injected into five or six sites in the left ventricular walls randomly. After the operation, the surgical wound was carefully sutured and gentamicin was given to prevent infection.

In situ detection of DNA fragmentation and nuclear condensation

Following the manufacturer's protocol, a TdT-mediated dUTP nick-end labeling (TUNEL) apoptosis detection kit (Keygen Biotech, China) was used to detect DNA fragmentation in the heart sections, and the percentage of apoptotic cells were quantified as the ratio of TUNEL-labeled cells to total cells in the heart fractions. Hoechst 33342 staining was performed to observe nuclear condensation of H_9C_2 cells.

Determination of the mitochondrial membrane potential and matrix swelling

To monitor the mitochondrial membrane potential ($\Delta\psi_m$), H_9C_2 cells were loaded with Rh123 (10 µg/ml, Sigma) or tetra-methylrhodamine ethyl ester (TMRE) (10 nmol/l, Invitrogen) at 37°C for 10 min. In addition, H_9C_2 cells were stained with 1 µmol/l Mitotracker Red (Invitrogen) at 37°C for 10 min for analysis of mitochondrial matrix swelling. Afterwards, the cells were washed three times and replaced by DMEM without Phenol Red. A laser scanning microscope (EVOS FL Auto, Life Technologies, Bothell, WA) was used to image the cells.

TEM and cell viability assay

To morphologically assess mitochondria in the hearts of rats, tissues were fixed with 2.5% cold glutaraldehyde for 30 min and then 1% osmium tetroxide was added. Uranyl acetate and lead citrate were used to stain ultrathin sections for observation under an electron microscope (JEM-1400, JEOL Ltd., Japan) in different visual fields.

In order to detect the cell viability of H_9C_2 cells after treatments, MTS was supplemented into cell cultures in 96-well plates and was incubated away from light for 2 h at 37°C. Then the absorbance was measured with a microplate reader (TECAN, Switzerland; 490 nm wavelength) and the viability of cardiomyocytes was determined by the assessing the absorbance of control and treatment groups.

Assessment of apoptosis by flow cytometric analysis

Cell apoptosis was assessed with an annexin V/propidium iodide (PI) apoptosis assay kit (BestBio, Shanghai, China). In short, the collected cells were washed twice (300–500 ***g***, 5 min) with ice-cold phosphate-buffered saline (PBS), and then the 1× binding buffer from the kit (4×10^6 cells/ml) was added to them. These mixtures were collected in a 2 ml culture tube, and then 5 µl annexin V and 10 µl PI were added into each tube in the dark for, respectively, 15 min and 5 min before the mixture was transferred into a 5 ml culture tube, which was used for testing. Finally, the cells were analyzed by flow cytometry (excitation at 488 nm; emission at 530 nm, EPICS XL, Beckman Coulter, USA). The proportion of apoptotic cells was determined as the percentage of positively stained cells.

Statistical analysis

Data are presented as means±s.e.m. Statistical analysis of two groups was performed with an unpaired Student's *t*-test, and one-way analysis of variance (ANOVA) with Bonferroni post-tests were used for multiple groups. A value of $P<0.05$ was considered statistically significant when analyzing the difference of groups.

Competing interests

The authors declare no competing or financial interests.

Author contributions

Conceptualization: L.L., J.L., P.L.; Methodology: L.L., Y.T., P.W., Z.G., Q.W., K.G., R.L.; Software: L.L., Y.T., P.W., Z.G.; Validation: L.L., J.L., P.L.; Formal analysis: L.L., J.L., P.L.; Investigation: L.L., P.W., Z.G., Q.W., K.G., R.L.; Resources: J.L., H.L., P.L.; Data curation: L.L., Y.T.; Writing - original draft: L.L.; Writing - review & editing: Y.T., J.L., P.L.; Visualization: L.L., P.W., Z.G.; Supervision: J.L., P.L.; Project administration: J.L., P.L.; Funding acquisition: J.L., H.L., P.L.

Funding

This research was supported by grants from the National Natural Science Foundation of China (81803521, 81872860, 81673433), Indigenous Innovative Research Team of Guangdong Province (2017BT01Y093), the National Major Special Projects for the Creation and Manufacture of New Drugs (2018ZX09301031-001), the Special Program for Applied Science and Technology of Guangdong Province (2015B020232009), the National Engineering and Technology Research Center for New Drug Druggability Evaluation (Seed Program of Guangdong Province, 2017B090903004), the Guangzhou Science and Technology Program Project (201604020121), Medical Scientific Research Foundation of Guangdong Province (A2018078), the Traditional Chinese Medicine Bureau of Guangdong Province (20191060) and the Natural Science Foundation of Guangdong Province (2017A030310542).

Supplementary information

Supplementary information available online at
http://jcs.biologists.org/lookup/doi/10.1242/jcs.228478.supplemental

References

Andersen, P., Tampakakis, E., Jimenez, D. V., Kannan, S., Miyamoto, M., Shin, H. K., Saberi, A., Murphy, S., Sulistio, E., Chelko, S. P. et al. (2018). Precardiac organoids form two heart fields via Bmp/Wnt signaling. *Nat. Commun.* **9**, 3140. doi:10.1038/s41467-018-05604-8

Chatterjee, K., Zhang, J., Honbo, N. and Karliner, J. S. (2010). Doxorubicin cardiomyopathy. *Cardiology* **115**, 155-162. doi:10.1159/000265166

Cheng, S.-L., Shao, J.-S., Behrmann, A., Krchma, K. and Towler, D. A. (2013). Dkk1 and MSX2-Wnt7b signaling reciprocally regulate the endothelial-mesenchymal transition in aortic endothelial cells. *Arterioscler. Thromb. Vasc. Biol.* **33**, 1679-1689. doi:10.1161/ATVBAHA.113.300647

Dawson, K., Aflaki, M. and Nattel, S. (2013). Role of the Wnt-Frizzled system in cardiac pathophysiology: a rapidly developing, poorly understood area with enormous potential. *J. Physiol.* **591**, 1409-1432. doi:10.1113/jphysiol.2012.235382

Di, M., Wang, L., Li, M., Zhang, Y., Liu, X., Zeng, R., Wang, H., Chen, Y., Chen, W., Zhang, Y. et al. (2017). Dickkopf1 destabilizes atherosclerotic plaques and promotes plaque formation by inducing apoptosis of endothelial cells through activation of ER stress. *Cell Death Dis.* **8**, e2917. doi:10.1038/cddis.2017.277

Duan, J., Gherghe, C., Liu, D., Hamlett, E., Srikantha, L., Rodgers, L., Regan, J. N., Rojas, M., Willis, M., Leask, A. et al. (2012). Wnt1/betacatenin injury response activates the epicardium and cardiac fibroblasts to promote cardiac repair. *EMBO J.* **31**, 429-442. doi:10.1038/emboj.2011.418

Foulquier, S., Daskalopoulos, E. P., Lluri, G., Hermans, K. C. M., Deb, A. and Blankesteijn, W. M. (2018). WNT signaling in cardiac and vascular disease. *Pharmacol. Rev.* **70**, 68-141. doi:10.1124/pr.117.013896

Garcia-Martín, A., Reyes-Garcia, R., García-Fontana, B., Morales-Santana, S., Coto-Montes, A., Muñoz-Garach, M., Rozas-Moreno, P. and Muñoz-Torres, M. (2014). Relationship of Dickkopf1 (DKK1) with cardiovascular disease and bone metabolism in Caucasian type 2 diabetes mellitus. *PLoS ONE* **9**, e111703. doi:10.1371/journal.pone.0111703

Gianni, L., Herman, E. H., Lipshultz, S. E., Minotti, G., Sarvazyan, N. and Sawyer, D. B. (2008). Anthracycline cardiotoxicity: from bench to bedside. *J. Clin. Oncol.* **26**, 3777-3784. doi:10.1200/JCO.2007.14.9401

Green, P. S. and Leeuwenburgh, C. (2002). Mitochondrial dysfunction is an early indicator of doxorubicin-induced apoptosis. *Biochim. Biophys Acta Mol. Basis Dis.* **1588**, 94-101. doi:10.1016/S0925-4439(02)00144-8

Huang, Y., Liu, L. and Liu, A. (2018). Dickkopf-1: current knowledge and related diseases. *Life Sci.* **209**, 249-254. doi:10.1016/j.lfs.2018.08.019

Hulmi, J. J., Nissinen, T. A., Räsänen, M., Degerman, J., Lautaoja, J. H., Hemanthakumar, K. A., Backman, J. T., Ritvos, O., Silvennoinen, M. and Kivelä, R. (2018). Prevention of chemotherapy-induced cachexia by ACVR2B ligand blocking has different effects on heart and skeletal muscle. *J. Cachexia Sarcopenia Muscle* **9**, 417-432. doi:10.1002/jcsm.12265

Hurlstone, A. F. L., Haramis, A.-P. G., Wienholds, E., Begthel, H., Korving, J., Van Eeden, F., Cuppen, E., Zivkovic, D., Plasterk, R. H. A. and Clevers, H. (2003). The Wnt/beta-catenin pathway regulates cardiac valve formation. *Nature* **425**, 633-637. doi:10.1038/nature02028

Kahn, M. (2014). Can we safely target the WNT pathway? *Nat. Rev. Drug Discov.* **13**, 513-532. doi:10.1038/nrd4233

Kim, K.-I., Park, K. U., Chun, E. J., Choi, S.-I., Cho, Y.-S., Youn, T.-J., Cho, G.-Y., Chae, I.-H., Song, J., Choi, D.-J. et al. (2011). A novel biomarker of coronary atherosclerosis: serum DKK1 concentration correlates with coronary artery calcification and atherosclerotic plaques. *J. Korean Med. Sci.* **26**, 1178. doi:10.3346/jkms.2011.26.9.1178

Li, M., Sala, V., De Santis, M. C., Cimino, J., Cappello, P., Pianca, N., Di Bona, A., Margaria, J. P., Martini, M., Lazzarini, E. et al. (2018). Phosphoinositide 3-Kinase Gamma Inhibition Protects From Anthracycline Cardiotoxicity and Reduces Tumor Growth. *Circulation* **138**, 696-711. doi:10.1161/CIRCULATIONAHA.117.030352

Merks, A. M., Swinarski, M., Meyer, A. M., Müller, N. V., Özcan, I., Donat, S., Burger, A., Gilbert, S., Mosimann, C., Abdelilah-Seyfried, S. et al. (2018). Planar cell polarity signalling coordinates heart tube remodelling through tissue-scale polarisation of actomyosin activity. *Nat. Commun.* **9**, 2161. doi:10.1038/s41467-018-04566-1

Niehrs, C. (2006). Function and biological roles of the Dickkopf family of Wnt modulators. *Oncogene* **25**, 7469-7481. doi:10.1038/sj.onc.1210054

Nusse, R. and Clevers, H. (2017). Wnt/beta-catenin signaling, disease, and emerging therapeutic modalities. *Cell* **169**, 985-999. doi:10.1016/j.cell.2017.05.016

Octavia, Y., Tocchetti, C. G., Gabrielson, K. L., Janssens, S., Crijns, H. J. and Moens, A. L. (2012). Doxorubicin-induced cardiomyopathy: from molecular mechanisms to therapeutic strategies. *J. Mol. Cell. Cardiol.* **52**, 1213-1225. doi:10.1016/j.yjmcc.2012.03.006

Ozhan, G. and Weidinger, G. (2015). Wnt/beta-catenin signaling in heart regeneration. *Cell Regen (Lond).* **4**, 3. doi:10.1186/s13619-015-0017-8

Ruiz-Villalba, A., Hoppler, S. and Van Den Hoff, M. J. B. (2016). Wnt signaling in the heart fields: Variations on a common theme. *Dev. Dyn.* **245**, 294-306. doi:10.1002/dvdy.24372

Sadahiro, T., Isomi, M., Muraoka, N., Kojima, H., Haginiwa, S., Kurotsu, S., Tamura, F., Tani, H., Tohyama, S., Fujita, J. et al. (2018). Tbx6 induces nascent mesoderm from pluripotent stem cells and temporally controls cardiac versus somite lineage diversification. *Cell Stem Cell* **23**, 382-95.e5. doi:10.1016/j.stem.2018.07.001

Santulli, G., Xie, W. J., Reiken, S. R. and Marks, A. R. (2015). Mitochondrial calcium overload is a key determinant in heart failure. *Proc. Natl. Acad. Sci. USA* **112**, 11389-11394. doi:10.1073/pnas.1513047112

Štěrba, M., Popelová, O., Vávrová, A., Jirkovský, E., Kovaříková, P., Geršl, V. and Šimůnek, T. (2013). Oxidative stress, redox signaling, and metal chelation in anthracycline cardiotoxicity and pharmacological cardioprotection. *Antioxid Redox Signal.* **18**, 899-929. doi:10.1089/ars.2012.4795

Takemura, G. and Fujiwara, H. (2007). Doxorubicin-induced cardiomyopathy from the cardiotoxic mechanisms to management. *Prog. Cardiovasc. Dis.* **49**, 330-352. doi:10.1016/j.pcad.2006.10.002

Ueland, T., Otterdal, K., Lekva, T., Halvorsen, B., Gabrielsen, A., Sandberg, W. J., Paulsson-Berne, G., Pedersen, T. M., Folkersen, L., Gullestad, L. et al. (2009). Dickkopf-1 enhances inflammatory interaction between platelets and endothelial cells and shows increased expression in atherosclerosis. *Arterioscler. Thromb. Vasc. Biol.* **29**, 1228-1234. doi:10.1161/ATVBAHA.109.189761

Umanskaya, A., Santulli, G., Xie, W., Andersson, D. C., Reiken, S. R. and Marks, A. R. (2014). Genetically enhancing mitochondrial antioxidant activity improves muscle function in aging. *Proc. Natl. Acad. Sci. USA* **111**, 15250-15255. doi:10.1073/pnas.1412754111

Wang, B., Liao, P. P., Liu, L. H., Fang, X., Li, W. and Guan, S. M. (2016). Baicalin and geniposide inhibit the development of atherosclerosis by increasing Wnt1 and inhibiting dickkopf-related protein-1 expression. *J. Geriatr Cardiol.* **13**, 846-854. doi:10.11909/j.issn.1671-5411.2016.10.013

Wo, D., Peng, J., Ren, D. N., Qiu, L., Chen, J., Zhu, Y., Yan, Y., Yan, H., Wu, J., Ma, E. et al. (2016). Opposing roles of Wnt inhibitors IGFBP-4 and Dkk1 in cardiac ischemia by differential targeting of LRP5/6 and beta-catenin. *Circulation* **134**, 1991-2007. doi:10.1161/CIRCULATIONAHA.116.024441

Xie, Z. D., Xia, W. Z. and Hou, M. (2018). Long intergenic non-coding RNA-p21 mediates cardiac senescence via the Wnt/beta-catenin signaling pathway in doxorubicin-induced cardiotoxicity. *Mol. Med. Rep.* **17**, 2695-2704. doi:10.3892/mmr.2017.8169

Yarana, C., Carroll, D., Chen, J., Chaiswing, L., Zhao, Y., Noel, T., Alstott, M., Bae, Y., Dressler, E. V., Moscow, J. A. et al. (2018). Extracellular vesicles released by cardiomyocytes in a doxorubicin-induced cardiac injury mouse model contain protein biomarkers of early cardiac injury. *Clin. Cancer Res.* **24**, 1644-1653. doi:10.1158/1078-0432.CCR-17-2046

Zhou, S., Starkov, A., Froberg, M. K., Leino, R. L. and Wallace, K. B. (2001). Cumulative and irreversible cardiac mitochondrial dysfunction induced by doxorubicin. *Cancer Res.* **61**, 771-777.